# A tool for designing water tanks for measuring hydroacoustic transducers

**Roman SALAMON** , **Jacek MARSZAL** , **Iwona KOCHAŃSKA**

Gdansk University of Technology Faculty of Electronics, Telecommunications and Informatics, Department of Sonar Systems, ul. Narutowicza 11/12, 80-233, Gdańsk, Poland

**Corresponding author:** Jacek MARSZAL, email: jacek.marszal@pg.edu.pl

**Abstract** Special water tanks are commonly used to measure the parameters of underwater acoustic systems. They must meet specific requirements, the fulfilment of which ensures very small but acceptable measurement errors. These requirements define the size of the tank and its shape as well as the strong attenuation of reflected waves. At the design stage, it is necessary to determine the impact of the tank structure on the measurement errors and to adapt it to the expected measurement methodology. The article presents a mathematical tool for designing such water tanks using the impulse response method. Contrary to the use of this method in architectural design, the presented method is here used to determine the measurement signals emitted by ultrasonic transmitting transducers and received by receiving transducers. The relationships are given between the parameters of the impulse response and the design parameters of the tank and the measurement system, as well as its transfer functions and sample measurement signals.

**Keywords:** hydroacoustic measuring tank, impulse response method, image-source method.

## 1. Introduction

A commonly applied step in designing, building, and operating both underwater acoustic equipment and systems are the measurements of transmitting and receiving ultrasound transducers. An important part of such measurements is performed in purpose-built measurement tanks. The limited size of such tanks lead to the generation of reflected signals, which may adversely affect the measurement accuracy. The reflection effects are ameliorated by inclining the tank walls, corrugating their surfaces, and lining them with low-reflection coefficient materials [1–6].

The paper presents a tank design tool that enables the determination of the effects of the tank shape and wave reflection coefficient on signals emitted by transmitting transducers and received by receiving transducers. The tool is a software designed to function in the MATLAB® environment, which uses the image-source method, frequently used in architectural acoustics. Unlike architectural acoustics, where this method is used to determine the spatial distribution of sound intensity in an entire room and the reverberation time, in a measurement tank the purpose of the test is to determine the relationship between the transmitted signal and the signal measured at the receiving transducer output. This is made possible by the impulse response method, which takes advantage of the convolution relationship between the input signal, output signal, and the impulse response of the test system.

In the method described in this paper the impulse response is a signal at the receiving transducer output sourced from a δ-Dirac impulse emitted by the transmitting transducer and arriving at the receiving transducer both directly and reflected from the tank walls. The method enables the determination of the impulse response for a tank of any shape, known wall reflection coefficients, and any sound source and receiver positions. By adjusting these parameters, it is possible to obtain an impulse response with a waveform desirable for the measurement methods to be used. The method can also be used to compare the measurement results with the theoretical calculation results.

## 2. Tank design

It is assumed that the tank is prism-shaped, with its shape and dimensions described by its vertex coordinates. The design process involves determining the dimensions of the rectangular surface of water between the tank walls, selecting its depth ($h$) and inclination angle ($\alpha$) of one of its surfaces. On this basis a pyramid is created with a rectangular base, intersected by a bottom plane with depth $h$, height

coordinates $x_w$ and $y_w$, and desired inclination $\gamma$. A tank built in this manner has inclined walls with different inclination angles. For convenience of notation, we assumed a Cartesian coordinate system symmetrical to the surface of the water. The tank construction method is illustrated in Fig. 1.
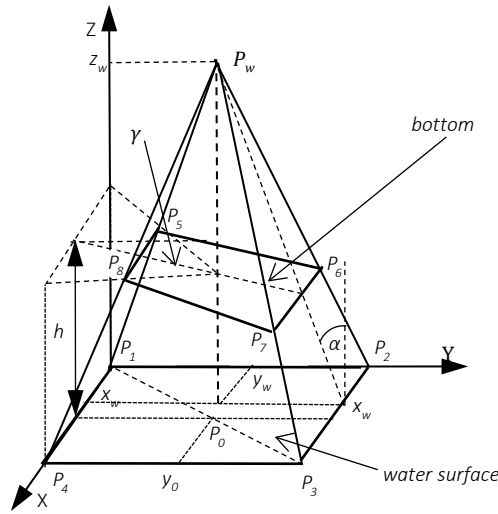


**Figure 1.** Constructing the tank.

Analytic geometry methods [7] are used for the tank structure design. Its purpose is to determine the equation coefficients of all the tank surfaces. The first step is to determine the coordinates of the rectangular water surface vertices: $P_1, P_2, P_3,$ and $P_4.$ Next, the apex coordinates $x_w$ and $y_w$, and inclination angle $\alpha$ for one of the walls are determined. For a wall with vertices $P_2, P_3,$ and $P_w$, the $z_w$ coordinate is:

$$z_w = (y_2 - y_w)\cot\alpha. \tag{1}$$

The side surfaces are defined as passing through three points. Consider a side surface passing through points $P_1(x_1=0, y_1=0, z_1=0)$ $P_2(x_2=0, y_2, z_2=0)$, and $P_w(x_w, y_w, z_w)$, designated as number 2. It is described by the following equation:

$$A_2x + B_2y + C_2z + D_2 = 0. \tag{2}$$

The plane equation coefficients are calculated using the following equations:

$$A_2 = \begin{vmatrix} y_2 - y_1 & z_2 - z_1 \\ y_w - y_1 & z_w - z_1 \end{vmatrix} \quad B_2 = -\begin{vmatrix} x_2 - x_1 & z_2 - z_1 \\ x_w - x_1 & z_w - z_1 \end{vmatrix} \quad C_2 = \begin{vmatrix} x_2 - x_1 & y_2 - y_1 \\ x_w - x_1 & y_w - y_1 \end{vmatrix}$$
$$D_2 = -(A_2x_1 + B_2y_1 + C_2z_1). \tag{3}$$

The coefficients of the other three side surfaces are calculated in a similar manner, substituting the corresponding vertex points of the water surface.

Next, the arbitrary tank depth, $h$, and its surface inclination, $\gamma$, are determined. The bottom surface equation results from the intersection of the pyramid side walls and the tank side surfaces. The bottom surface passes through points with coordinates $(x_1, y_1, h)$, $(x_4, y_4, h)$, and $(x_0, y_0, z_0)$, where $x_0, y_0$ are the coordinates of intersection with the water surface rectangle, while $z_0$ is:

$$z_0 = h - y_2 tg\gamma. \tag{4}$$

The bottom surface equation is:

$$A_6x + B_6y + C_6z + D_6 = 0. \tag{5}$$

and its coefficients are calculated using equations with the Eq. (3),

The unknown coordinates, $P_5,...,P_8$, satisfy the systems of the three equations of their corresponding surfaces. For example, point $P_5$ satisfies the following system of equations:

$$A_2x + B_2x + C_2x + D_2 = 0 \quad A_5x + B_5x + C_5x + D_5 = 0 \quad A_6x + B_6x + C_6x + D_6 = 0, \tag{6}$$

where indices 2 and 5 indicate the surfaces shown in Fig. 1.

The coordinates of point $P_5(x_5, y_5, z_5)$ are calculated with the following matrix equation:

$$\begin{bmatrix} x_5 \\ y_5 \\ z_5 \end{bmatrix} = \begin{bmatrix} A_2 & B_2 & C_2 \\ A_5 & B_5 & C_5 \\ A_6 & B_6 & C_6 \end{bmatrix}^{-1} \begin{bmatrix} -D_2 \\ -D_5 \\ -D_6 \end{bmatrix}. \tag{7}$$

### 3. Image-source method

The image-source method assumes that a wave reflected from a flat surface is emitted by a source that is symmetrical to the actual source relative to the reflecting surface. On subsequent reflections from other planes, the image sources act as actual sources with new image sources appearing.

The general notation defined above for a certain tank surface takes the following form:

$$Ax + By + Cz + D = 0. \tag{8}$$

The coefficients $A$, $B$, and $C$ are the coordinates of a vector perpendicular to the plane in question. The line on which the actual source and the image source lie has the direction of this vector. Designating the source coordinates as $P_z(x_z, y_z, z_z)$, its equation can be written as:

$$\frac{x - x_z}{A} = \frac{y - y_z}{B} = \frac{z - z_z}{C}. \tag{9}$$

The image source also lies on the line defined by Eq. (9), therefore:

$$\frac{x_p - x_z}{A} = \frac{y_p - y_z}{B} = \frac{z_p - z_z}{C}, \tag{10}$$

and the plane puncture points $P_c(x_c, y_c, z_c)$, which satisfies the equation:

$$\frac{x_c - x_z}{A} = \frac{y_c - y_z}{B} = \frac{z_c - z_z}{C} = k. \tag{11}$$

It follows from the above equations that:

$$x_c = x_z + pA \quad y_c = y_z + pB \quad z_c = z_z + pC, \tag{12}$$

where $k$ and $p$ are auxiliary variables. The puncture point satisfies the plane Eq. (8), thus:

$$A(x_z + pA) + B(y_z + pB) + C(z_z + pC) + D = 0. \tag{13}$$

This leads to:

$$Ax_z + By_z + Cz_z + D + k(A^2 + B^2 + C^2) = 0, \tag{14}$$

and:

$$p = -\frac{Ax_z + By_z + Cz_z + D}{A^2 + B^2 + C^2}. \tag{15}$$

By substituting the value of coefficient $p$ to Eq. (12), the coordinates of the puncture point $P_c$ can be calculated. This point is the middle of a section between the actual source and the image source, therefore:

$$x_p = x_z + 2x_c \quad y_p = y_z + 2y_c \quad x_p = z_z + 2z_c. \tag{16}$$

These are the coordinates of the image source.

The distance of the image source $Pp$ from the hydrophone (receiving transducer) is:

$$R = \sqrt{(x_h - x_z)^2 + (y_h - y_z)^2 + (z_h - z_z)^2}, \tag{17}$$

where $(x_h, y_h, z_h)$ are the coordinates of the hydrophone.

These can be used to determine the delay of the reflected signal received by the hydrophone, relative to the signal emitted by the source. The delay is:

$$\tau = \frac{R}{c}, \tag{18}$$

where $c$ is the acoustic wave speed in water.

Amplitude $S_h$ of the pressure received by the hydrophone, assuming no absorption, is:

$$S_h = \beta S_z \frac{R_1}{R}, \tag{19}$$

where $S_z$ is the pressure amplitude of a wave emitted by a source, measured at distance $R_1$ from the source. The symbol $\beta$ denotes a pressure coefficient of reflection from the tank surface. In the numerical calculation results presented later here, it is always assumed that $P_z$ = 1 Pa, and $R_1$ = 1 m.

The software written for the MATLB® environment determines the signals received by a hydrophone as samples representing δ-Dirac pulses, whose sequence forms the impulse response $k(t)$ when a transmitted pulse has a unit amplitude. A sample impulse response that includes the first reflection is shown in Fig. 2 and a second reflection in Fig. 3. The water surface has a length of 12 m, width of 10 m, the tank height is 8 m, the apex coordinates are $x_w$ = 5 m and $y_w$ = 6 m, and the inclination angles are $\alpha$ = 10° and $\gamma$ = 5°. The coordinates of the non-directional sound source are $P_z(4, 5, 3)$, and those of the hydrophone are $P_h(4, 9, 3)$. It is assumed that the reflection coefficient for all walls is $\beta$ = 0.5.
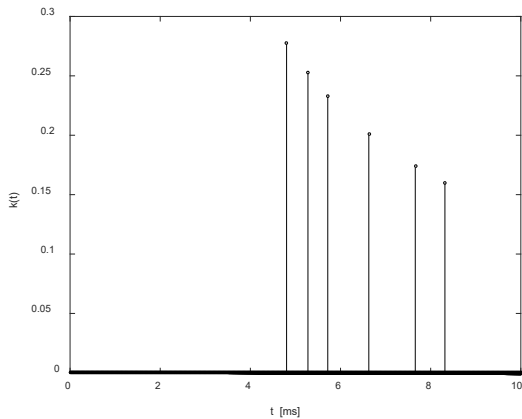


**Figure 2.** Impulse response for the first reflection.
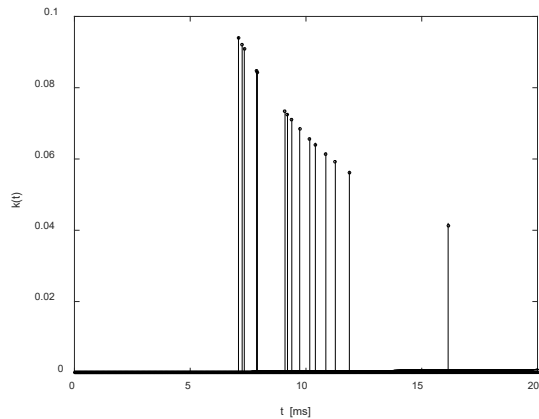


**Figure 3.** Impulse response for the second reflection.

Subsequent reflections are calculated by assuming that the actual sources are the image sources calculated previously. The MATLAB® environment software limits itself to four reflections, as any further ones have practically no effect on the impulse response. This is illustrated below in the Fig. 4. For simplicity, the Fig. 4 shows a cross-section of the tank as a regular tetragon, and indicates the sound source (S) and hydrophone (H). The calculated image source relative to surface 1, marked as $P_1$, image source secondary to the first one relative to surface 2, marked as $P_{12}$, and further image sources relative to surface 2 – $P_{122}$, relative to surface 3 - $P_{123}$, and relative to surface 4 - $P_{1234}$. The indices denote reflections from the surfaces of the corresponding numbers. The numbers of digits in the index specifies the sequence and number of consecutive reflections.
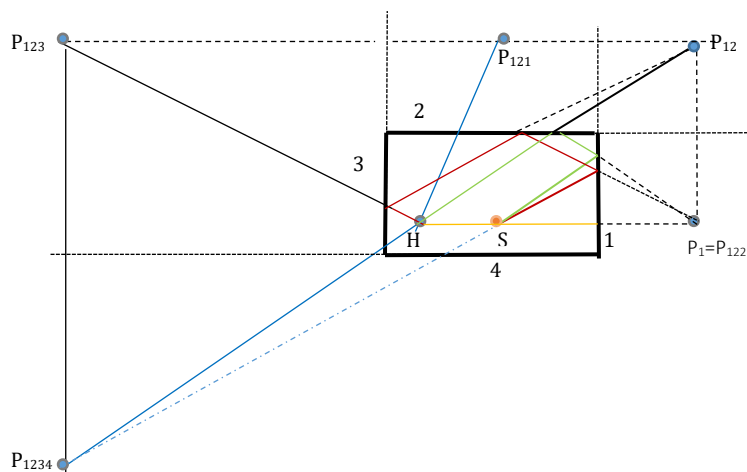


**Figure 4.** Secondary image sources and reflected wave paths.

The first reflection occurs off source $P_1$ and is marked in orange. The wave path from source $P_{12}$ is marked in green. Source $P_{121}$ is a false source, it does not satisfy the criterion of equality of the path from the image source to the hydrophone and the path of reflected waves while maintaining equality of angles

of incidence and reflection. Source $P_{122}$ has the position of source $P_1$, so it should be eliminated. The wave path from the image source $P_{123}$ is marked in red. Source $P_{1234}$ is a false source, as the path from it to hydrophone $H$ is shorter than the path to source $S$.

The example shown demonstrates that not all the image sources set the wave paths on subsequent reflections. It is therefore necessary to establish criteria for eliminating false image sources. A detailed analysis, which is not discussed here for lack of space, has demonstrated that there are three causes for the occurrence of false sources. These are: incorrect sequence of reflections from individual walls, failure of the line connecting the image source and the hydrophone to intersect the right wall, and the presence of an image source inside the tank.

The first criterion for eliminating false sources can be written as follows for four reflections, following the image source notation $P_{nmkl}$:

- second reflection　　　　　$n = m,$
- third reflection　　　　　　$n = m \cup n = k \cup m = k,$
- fourth reflection　　　　　$n = m \cup n = k \cup n = l \cup m = k \cup m = l \cup k = l,$

where n, m, k, l denote the wall numbers (1,...6) of consecutive reflections.

This notation leads to a general conclusion that the different variations without repetitions from a six-element set (wall numbers) of a 1, 2, 3, and 4-element set are not eliminated. Their number is, in the above order, 1, 30, 120, and 360.

In the second criterion, the equation of the line connecting the image source $P_p(x_p,y_p,z_p)$ with the hydrophone $P_h(x_h,y_h,z_h)$ is calculated:

$$\frac{x - x_p}{x_h - x_p} = \frac{y - y_p}{y_h - y_p} = \frac{z - z_p}{z_h - z_p} = p. \tag{20}$$

Thus:

$$x = k(x_h - x_p) + x_p \quad y = k(y_h - y_p) + y_p \quad z = k(z_h - z_p) + z_p. \tag{21}$$

One wall of the tank is described with the following equation:

$$Ax + By + Cz + D = 0. \tag{22}$$

The x, y, z coordinates are the coordinates of the puncture point if they satisfy the above equations. Substituting Eq. (21) to the above equation produces the following:

$$p(Aa + Bb + Cc) = -(D + Ax_p + By_p + Cz_p), \tag{23}$$

and therefore

$$p = -\frac{D + Ax_p + By_p + Cz_p}{Aa + Bb + Cc}. \tag{24}$$

The puncture point coordinates x, y, and z can be calculated using Eq. (21).

Next the position of the puncture point is checked against each of the four lines delimiting the corresponding tank wall. The check method is illustrated below in the Fig.5, where the surface is placed in an X, Y coordinate system for simplicity.
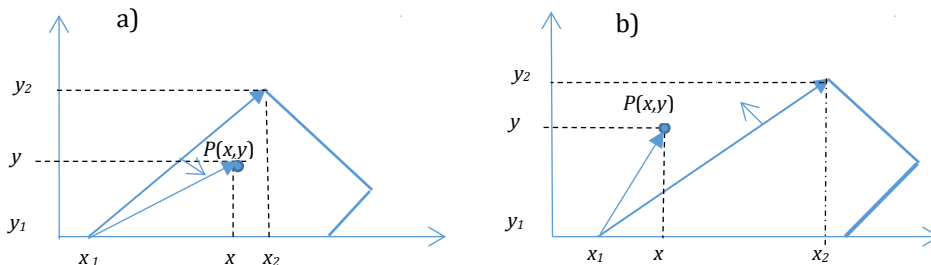


**Figure 5.** Calculation of the puncture point $P(x,y)$: a) the point lies within the tank wall,
b) the point lies outside the wall.

Now let us calculate vector $\vec{p}(a_x, a_y, a_z)$ and vector $\vec{p_p}(b_x, b_y, b_z)$, where $a_x = x_2\text{-}x_1$, $a_y = y_2\text{-}y_1$, $a_z = z_2\text{-}z_1$, $b_x = x_1\text{ -}x_c$, $b_y = y_1\text{ -}y_c$, $b_z = z_1\text{- }z_c$, and the vector product $\vec{w} = \vec{p} \times \vec{p_p}$, which takes the following form in a matrix notation:

$$\begin{bmatrix} w_x \\ w_y \\ w_z \end{bmatrix} = \begin{vmatrix} \vec{\imath} & \vec{\jmath} & \vec{k} \\ a_x & a_y & a_z \\ b_x & b_x & b_x \end{vmatrix}. \tag{25}$$

The criterion for the puncture point to be located inside the wall is a specific vector sense $\overrightarrow{w}$.

The following procedure is used to eliminate image sources that lie inside the tank. The actual source is certain to lie inside the tank, on specific sides of its walls. Let the source have the coordinates $x_s$, $y_s$, $z_s$, the image source $x, y, z$. and one tank wall have the equation parameters $A, B, C, D$.

A vector with the coordinates [$A, B, C$] and vector [$x_z, y_z, z_z$] has its beginnings in the centre of the coordinate system. Calculate the scalar product of the two vectors and complete it with $D$:

$$Ax_z + By_z + Cz_z + C = a. \tag{26}$$

Do the same for the vector of the image source [$x\,y\,z$] to be checked:

$$Ax + By + Cz + D = b. \tag{27}$$

This operation is done for all six planes, producing the following sequences of numbers:

$$a = [a_1\,a_2\,a_3\,a_4\,a_5\,a_6], \tag{28}$$

$$b = [b_1\,b_2\,b_3\,b_4\,b_5\,b_6]. \tag{29}$$

Put 1 in place of positive numbers, and 0 in place of negative ones. For example, this gives:

$$a_b(n) = [1\,0\,1\,1\,0\,1], \tag{30}$$

$$b_b(n) = [1\,0\,1\,1\,0\,1]. \tag{31}$$

The properties of the scalar product demand that if $a_b(n)=b_b(n)$, then the points lie on the same side of the plane. For all walls, the criterion for eliminating a potential false image source is therefore: $a_n=b_n$.

## 4. Impulse response of the tank

The method described above makes it possible to determine the impulse response of the tank for any dimensions, wall inclinations, reflection coefficients, sound source positions, and receiving transducers. The effects of the above factors on the impulse response parameters can be demonstrated on the example of a tank with the assumed constant surface. The point of reference is a measurement tank the shape of a cuboid with the dimensions 10x12x8 m, with walls that perfectly reflect acoustic waves, ($\beta = 1$).
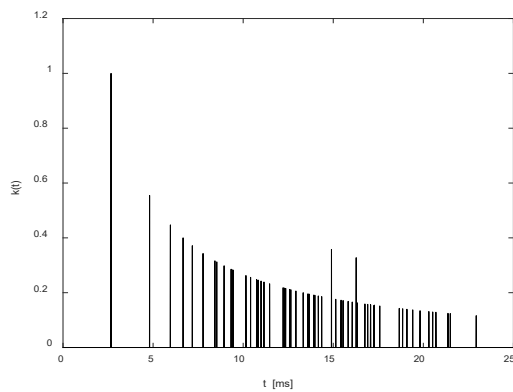


**Figure 6.** Impulse response for a rectangular prism-shaped tank with full wave reflections.
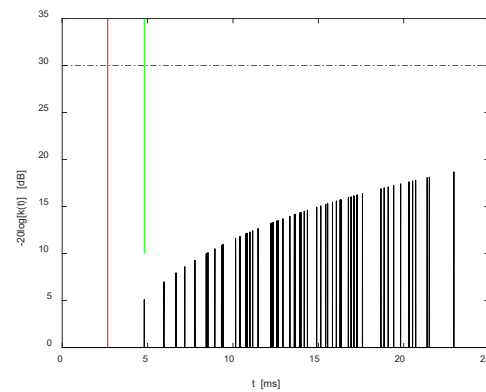
**Figure 7.** Attenuation of reflected pulses from Fig. 6.

The source and hydrophone coordinates are the same as in Fig. 3. The impulse response is shown in Fig. 6. It is normalised relative to the size of the pulse received directly by the hydrophone (first pulse). Figure 7 hows the pulse attenuation in decibels, which is used to determine the reverberation time. In hydroacoustic measurements, performed using the impulse method, it is assumed that another measurement impulse can be generated, when the reflected signals are attenuated by at least 30 dB. The reverberation time is determined according to this criterion.As can be seen in Fig. 7, the reverberation time is longer than the time of appearance of the last of the four reflections. The situation is radically improved when walls with a

lower reflection coefficient are used, which in the figures below (Fig. 8. and Fig. 9) is $\beta$=0.5. Reverberation time (shown in the Fig. 9), is now 18.7 ms. Within the time span between the direct pulse reception (marked in red) and the moment when the first reflected pulse appears (marked in green), there exist free field conditions in which measurements by the pulse method can be made. In the situation shown in the Fig. 9, this time is $\tau_s$= 2.4 ms. To achieve a long time $\tau_s$, the source and the hydrophone should be positioned at the shortest possible distance from each other, and the hydrophone should be as far as possible from the closest tank wall.
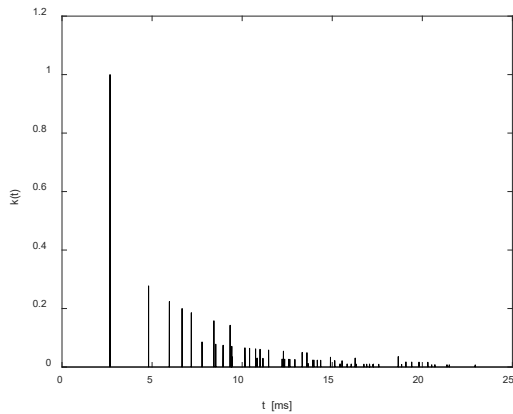


**Figure 8.** Impulse response for the tank from Fig. 6 at reflection coefficient $\beta$=0.5.
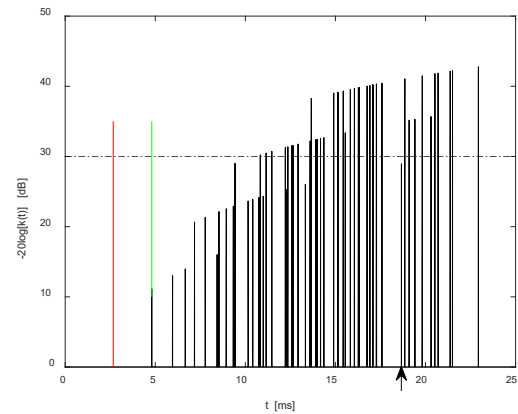
**Figure 9.** Attenuation of reflected pulses from Fig. 8.

Row A in the summary presented below in Tab. 1., shows the reverberation times $\tau_p$ at consecutive reflection coefficient values $\beta$. In the same table, row B shows reverberation time changes for walls inclined at angles $\alpha$=10°, $\gamma$=5°. In either case, the apex of the pyramid is positioned centrally. In the last row C, the position of the pyramid apex is shifted in the $x$ by 1 m, and in the $y$ direction by 2 m.

**Table 1.** Reverberation time as a function of the reflection coefficient $\tau_p(\beta)$ [ms].

|   | $\beta$ | | | | | | |
|---|------|------|------|------|------|------|------|
|   | 0.7  | 0.6  | 0.5  | 0.4  | 0.3  | 0.2  | 0.1  |
| A | 20.3 | 18.7 | 18.7 | 13.3 | 9.3  | 9.3  | 8.4  |
| B | 19.6 | 18.0 | 16.1 | 11.9 | 8.3  | 8.3  | 8.3  |
| C | 20.2 | 18.2 | 16.6 | 12.0 | 12.2 | 8.2  | 8.2  |

The change in reverberation time length is not systematic, because as the reflection coefficient drops, earlier reflections have a more pronounced effect due to the resultant reflection coefficient being a lower power of reverberation time. Furthermore, pulses of different heights cross the stated threshold at the same time. The Table 1 shows the beneficial effect of wall inclination on reverberation time, while shifting the cylinder apex causes deformations in the tank shape and slightly increases the reverberation time.

The effects of tank parameters and source and hydrophone position on the impulse response shown here do not, for obvious reasons, provide information on all possible situations, although they do point to the observed tendencies that may be useful for measurement tank designers.

## 5. Tank transmission function

The transmission function $K(f)$ describes the ratio of the sinusoidal signal received by the hydrophone to the signal emitted by its source. It is equal to the Fourier transform of the impulse response:

$$K(f) = |\mathfrak{I}\{k(t)\}|. \tag{32}$$

The transmission function makes it possible to assess the measurement error of a continuous sinusoidal signal depending on tank construction and the positioning of the sound source and hydrophone. It is characterised by an average value $\bar{K}$, standard deviation $\sigma$, and amplitude measurement mean                                                                                                                              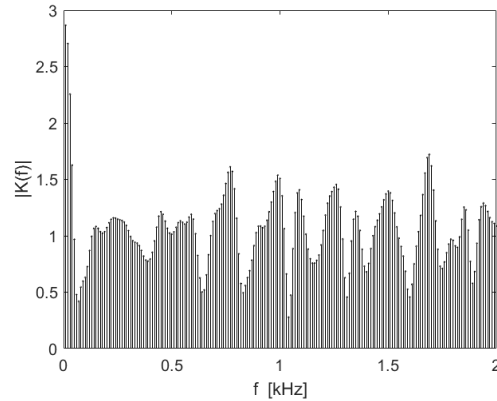                            error $e$ resulting from the corrugation of the transmission function. This error is calculated as follows:

$$e = (\overline{K} - \sigma)/\overline{K}. \tag{33}$$

Figure 10 shows a sample transmission function for the considered cuboid tank, when – in accordance with the recommendations mentioned earlier – the source and hydrophone are positioned centrally, and the distance between them is reduced. The coordinates of the sound are $P_s(5, 5, 4)$, and those of the hydrophone are $P_h(5.1, 7.1, 4.1)$. The free field time, measured using the impulse response, is $\tau_s$ = 4 ms and is almost twice as long as in the example shown in Fig. 6. The reflection coefficient for all walls is $\beta$ = 0.5. Fig. 11 shows a low frequency portion of the transmission function in Fig. 10.

The parameters of the transmission function shown in Fig. 10 are not constant. At frequencies up to approx. 100 Hz, the error $e$ = 2.8 dB, while in the rest of the range it is $e \cong 2.1$ dB.
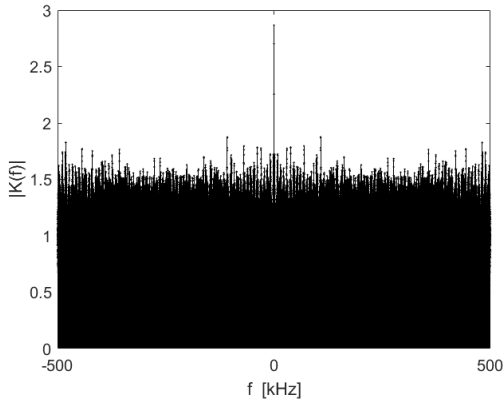


| **Figure 10.** Transmission function of the source - hydrophone system. | **Figure 11.** Transmission function of Fig. 10. in the low frequency range. |

The Table 2 below summarises the amplitude measurement error $e$ calculation results and reverberation time as a function of reflection coefficient $\beta$. In rows A they refer to a cuboid tank with the source and hydrophone positions provided above, in rows B the tank has walls inclined at angles $\alpha$ = 10° and $\gamma$ = 5°, and in rows C the pyramid apex is additionally shifted in the $x$ direction by 1 m, and in the $y$ direction by 2 m.

**Table 2.** Amplitude measurement error $e$ and reverberation time $\tau_p$.

| | | $\beta$ | | | | | | |
|---|---|---|---|---|---|---|---|---|
| | | 0.7 | 0.6 | 0.5 | 0.4 | 0.3 | 0.2 | 0.1 |
| A | $e$ [dB] | 3.5 | 2.7 | 2.1 | 1.5 | 1.1 | 0.7 | 0.3 |
| A | $\tau_p$ [ms] | 17.4 | 14.6 | 10.8 | 8.1 | 8.1 | 8.2 | 0 |
| B | $e$ [dB] | 4.3 | 3.3 | 2.4 | 1.7 | 1.2 | 0.8 | 0.4 |
| B | $\tau_p$ [ms] | 15.1 | 14.5 | 10.2 | 6.8 | 6.8 | 6.8 | 0 |
| C | $e$ [dB] | 4.3 | 3.2 | 2.4 | 1.7 | 1.2 | 0.8 | 0.4 |
| C | $\tau_p$ [ms] | 15.1 | 15.0 | 10.2 | 7.0 | 7.0 | 7.0 | 0 |

The results presented in the table show the effect of lowering the reflection coefficient $\beta$ on the reduction of amplitude measurement error $e$ resulting from the corrugation of the transmission function, and on shortening of reverberation time $\tau_p$. In comparison with Table 1., it can be seen that the central position of the measurement system and reducing the distance between the sound source and the hydrophone greatly reduces the reverberation time. It is worth noticing that tank wall inclination slightly increases the reverberation time and increases error $e$.
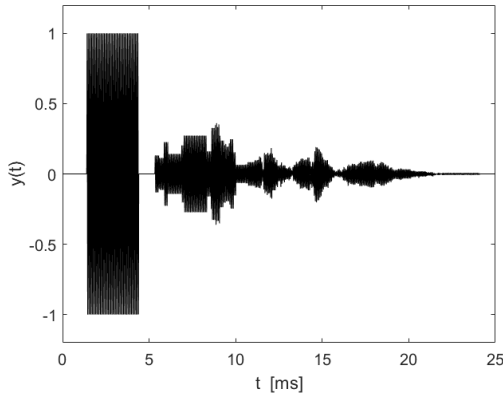
## 6. Measurement signals

When we have the impulse response, it is possible to calculate the signals received by the hydrophone at any excitation. The signal received $y(t)$ at excitation $x(t)$ is calculated using the equation:

$$y(t) = \int_0^t k(\tau)x(t - \tau)d\tau. \tag{34}$$

One method of ultrasound transducer measurement is to use sinusoidal signals with a rectangular envelope. It is the most convenient when pulse duration $\tau$ is shorter than free field time $\tau_s$. A signal of such a pulse received by the hydrophone is shown in Fig. 12. The measurement is not marred by errors caused by wave reflections from the tank walls. For longer pulse durations, as shown in Fig. 13, amplitude measurements can only be made during the free field time.



**Figure 12.** Received sinusoidal signal with a rectangular envelope, $\tau<\tau_s$.
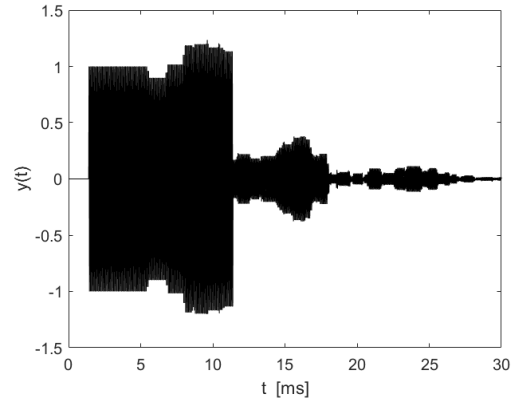
**Figure 13.** Received sinusoidal signal with rectangular envelope, $\tau>\tau_s$.

Pulse measurements have a lower limit imposed by frequency. This is due to the transient state occurring at the front of the pulse, when its spectrum is limited as a result of filtration. It is necessary to maintain a stationary state in which the signal amplitude measurements can be made. This is illustrated in the figures below. Figure 14 shows a received signal with a frequency of 5 kHz and duration $\tau = 4$ ms. A pulse with a rectangular envelope is filtered with a second-order Butterworth filter, with a transmission band width of 1 kHz (20% of the carrier frequency typical for piezoceramic transducers). The direct signal reception time is 1.4 ms, free field time is 4.0 ms, and the first reflected signal appears after 5.4 ms. It was assumed that amplitude measurements would be made in the time range from 4 ms to 5 ms, where the transient state can be ignored. Nevertheless, the measurement result is subject to a minor error. The maximum amplitude is 1.0022, the effective value is 0.70805, so amplitude error relative to 1 is 0.018941 dB and standard deviation error is 0.013 dB.
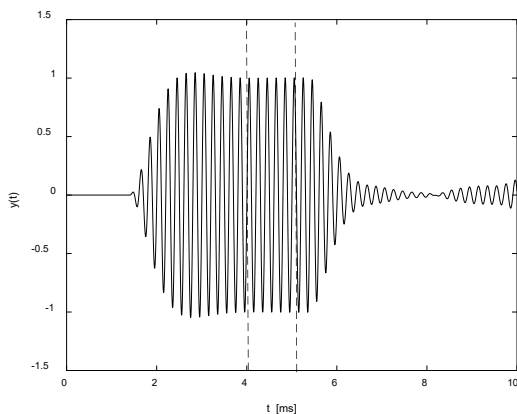


**Figure 14.** Pulse received after filtration, $f = 5$ kHz.
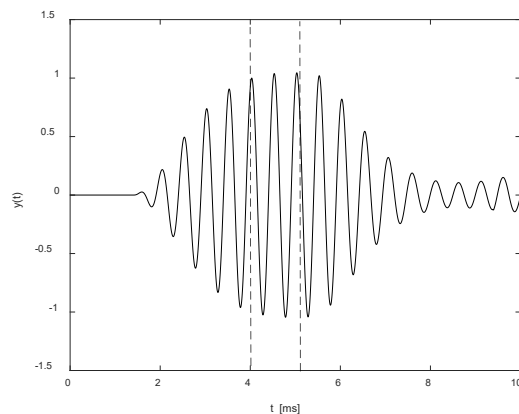
**Figure 15.** Pulse received after filtration, $f = 2$ kHz.

In Figure 14 it was assumed that the pulse carrier frequency is 2 kHz and pulse duration is 4 ms. The bandwidth was reduced to 0.4 kHz, which is 20% of the carrier frequency. The measurement performed again in the 4 ms to 5 ms time range carries the following errors: amplitude error relative to 1 is 0.3 dB and standard deviation error is 0.26 dB. A tendency for increasing measurement error as signal frequency lowers is visible.Reducing the pulse duration due to a shorter free field time and increasing the transient

state duration caused by a higher order of filtration necessitates increasing the sinusoidal signal frequency of the pulse. This is illustrated below in the Fig. 16. and the Fig. 17.

The continuous sinusoidal signal measurement method is not useful, which is a direct consequence of the transmission function form discussed in the preceding section. The significant corrugation of this function causes a significant spread in the received signal amplitude, depending on the signal frequency selected.

A solution may be to use signals with linear frequency modulation (LFM) and linear correlation reception modulation. After calculations are performed using Eq. (32), the following correlation function is calculated:

$$z(t) = \int_0^t y(\tau)x(t+\tau)d\tau. \tag{35}$$

This is illustrated in the figures made for a cuboid tank with a centrally located apex and source coordinates $P_s(5, 5, 4)$, hydrophone coordinates $P_h(5.1, 7.1, 4.1)$, and reflection coefficient β = 0.5. Reverberation time is $\tau_p$ = 8 ms, and free field time is $\tau_s$ = 4 ms. LFM signal middle frequency is 2kHz, its spectrum width is 0.4 kHz, and duration is 0.1 s. The measurement error of the correlation function maximum value $z(t)$ relative to the maximum value determined for the free field (β = 0) is 0.012 dB, so it is an error at the level of the numerical calculations error. It is worth noticing that the error achieved with the pulse measurement method is much greater at 0.3 dB (Fig. 13).
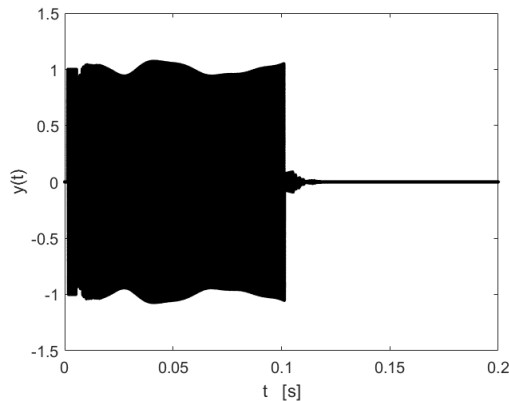


**Figure 16.** Received LFM signal.
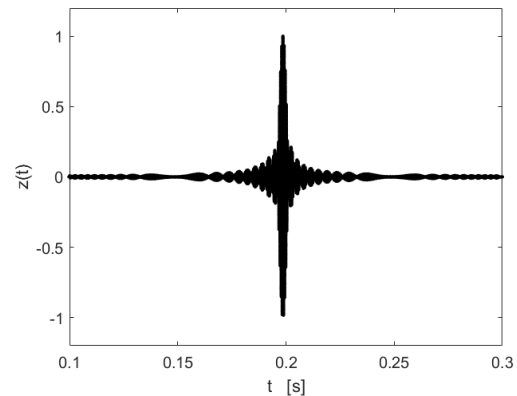


**Figure 17.** Correlation function of the received LFM signal.

The calculations performed demonstrated that increasing the LFM signal middle frequency does not increase the measurement error. However, lowering this frequency does increase the error. For example, for a middle frequency of 1 kHz, spectrum width of 0.2 kHz, and pulse duration of 0.1 s, the measurement error is 0.5 dB.

## 7. Conclusions

The above analysis of measurement signals using the impulse response method enables the following design recommendations to be made:
- ensure as large dimensions of the tank as possible
- ensure as low wave reflection coefficient as possible for the walls
- use a moderate wall inclination angle or forgo inclination altogether
- use a central position for the source - hydrophone line and a relatively small distance between the two.

It was demonstrated that the impulse response method enables the calculation of the measurement signals, and consequently verification of the measurement method used. Limitations of the impulse measurement method were discussed, in particular the relationships between the impulse response parameters and the lower frequency and pulse duration. Spectral analysis confirmed that the continuous sinusoidal wave measurement method is correctly ruled out. It was demonstrated that the use of signals with a linear frequency modulation in the measurements provides very low measurement errors in a broad range of frequencies and for relatively high coefficients of reflection from the tank walls.

The methods presented above can also be used to model the properties of the hydroacoustic channel in order to study the transmission properties in underwater telecommunications [8].

**Acknowledgments**

**Additional information**

The authors declare: no competing financial interests and that all material taken from other sources (including their own published works) is clearly cited and that appropriate permits are obtained.

**References**

1. A. Berkhout, D. Vries, M. Boone; A new method to acquire impulse responses in concert halls;
   J. Acoust. Soc. Am., 1980, 68(1), 179–183; DOI:10.1121/1.384618
2. IEC 60565-1:2020-0; International Standard: Underwater acoustics – Hydrophones – Calibration of hydrophones – Part 1: Procedures for free-field calibration of hydrophones, 2020
3. ISO 18233:2006; International Standard: Acoustics – Application of new measurement methods in building and room acoustics, 2006
4. A. Kulowski; Akustyka sal. Zalecenia projektowe dla architektów (in Polish); Wydawnictwo Politechniki Gdańskiej, Gdańsk 2011
5. N. Cochard, J. Lacoume, Y. Gabillet; Underwater Acoustic Noise Measurement in Test Tank; IEEE Journal of Oceanic Engineering, 2000, 25(4), 516–522; DOI: 10.1109/48.895359
6. J. Dong and P. Tian; Review of underwater sound absorption materials; ICEMEE 2020 Conf.; Tian 2020 IOP Conf. Ser.: Earth Environ. Sci., 2020, 508, 012182; DOI: 10.1088/1755-1315/508/1/012182
7. G. Landi, A. Zampini; Linear Algebra and Analytic Geometry for Physical Sciences;
   Springer International Publishing, 2018
8. I. Kochańska, R. Salamon, J. Schmidt, A. Schmidt; Study of the Performance of DSSS UAC System Depending on the System Bandwidth and the Spreading Sequence; Sensors, 2021, 21(7), 2484;
   DOI: 10.3390/s21072484